Computer Engineering and Applications Vol. 14, No. 2, June 2025

Improving Low-Cost Single-Phase Inverter Performance using DRL-Based Control System: Experimental Validation

Muhammad Irfan Jambak[1,*], Muhammad Abu Bakar Sidik[1], Noer Fadzri Perrdana Dinata[1,2]

[1]*Department of Electrical Engineering,Faculty of Engineering,Universitas Sriwijaya*
[2]*Department of Electrical Engineering, Faculty of Science and Technology, Universitas Bina Darma*
**corresponding author email: irfjambak@unsri.ac.id*

ABSTRACT

This paper presents the improvement of a low-cost, single-phase pure sine wave inverter controlled by a deep reinforcement learning (DRL) agent. The study addresses the challenge of lacking performance of low-cost inverter, which is primarily due to the stability requirements of conventional control strategies. A DRL-based control approach is proposed to enhance voltage and frequency stability while reducing the need for extensive manual tuning. The system is validated through both simulation and experimental verification in a microgrid islanded configuration. The results demonstrate that the DRL-based inverter effectively maintains 220 V_{RMS} at 50 Hz, achieving a stable root mean square voltage of 219.8 V, and a total harmonic distortion (THD) below 8%. The use of DRL making it an attractive solution for renewable energy systems, off-grid applications, and rural electrification. This study highlights the feasibility of DRL in power electronics and suggests that further optimization of training generalization and computational efficiency could enhance real-time and grid-tied deployment. The findings contribute to the advancement of intelligent inverter control, offering an alternative for next-generation microgrid and distributed energy systems.

Keywords: Deep Reinforcement Learning, Single-Phase Inverter, Microgrid, Voltage Stability, Frequency Stability.

1. INTRODUCTION

Pure sine wave inverters are essential for stable power delivery in microgrid applications[1], [2], particularly in islanded configurations where grid support is unavailable [3]. However, commercial pure sine wave inverters are often expensive due to the complexity of their control systems, which require precise voltage and frequency regulation [4].

To address this issue, this study proposes a method to improved sine wave quality of a low-cost, single-phase inverter controlled by a DRL-Agent. Unlike traditional controllers, which rely on predefined mathematical models and fixed parameters [5], [6], [7], DRL enables an adaptive control strategy that learns optimal responses through interaction with the system. Previous simulations have demonstrated that a trained DRL agent can stabilize inverter voltage under fluctuating loads [8], [9]. However, experimental validation is necessary to confirm its practical feasibility [8].

This paper presents an experimental verification of the DRL-based inverter for a microgrid islanded configuration. The system consists of a voltage regulator, gate driver, and metering system to assess the inverter's output stability. The objective is to demonstrate that a DRL-based controller can achieve stable 220 V_{rms}, 50 Hz output, offering a cost-effective alternative to conventional pure sine wave inverters.

2. METHODOLOGY

2.1 SYSTEM OVERVIEW

The proposed system consists of a single-phase inverter controlled by a DRL voltage regulator. The experimental setup, as illustrated in Figure 1, includes a 12V DC power source, an inverter circuit, a gate driver, a voltage regulator, and a metering/oscilloscope to monitor the output waveform. The DRL-based controller is responsible for dynamically adjusting the inverter's switching signals to maintain a stable 220 V_{rms}, 50 Hz output.

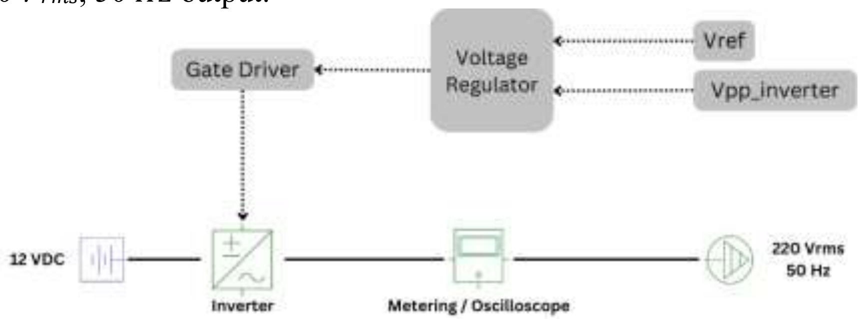

FIGURE 1. Single-line diagram (SLD) of the off-grid inverter configuration to be verified at the laboratory scale. The power source is a 12 VDC 10 Ah battery, with the expected output of 220 VAC 50 Hz single-phase voltage.

2.2 DRL-BASED CONTROL STRATEGY

In Figure 2, the controller's architecture is illustrated. The Phase-Lock-Loop (PLL) block diagram uses measurements from the grid to calculate the microgrid's voltage [10], [11] and frequency [12], [13]. The angle is used for synchronization in the inverse $dq0$ calculation, with voltage and frequency serving as state observations for the DRL agent. The output from the inverse $dq0$ calculation determines the switching frequency and duty cycle for the PWM generator, which is connected to a 6-pulse gate multiplexer driving the inverter. The inverter generates a sinusoidal waveform, which is processed through microgrid metering. A second PLL then compares this waveform to the setpoint to obtain the control system error value.

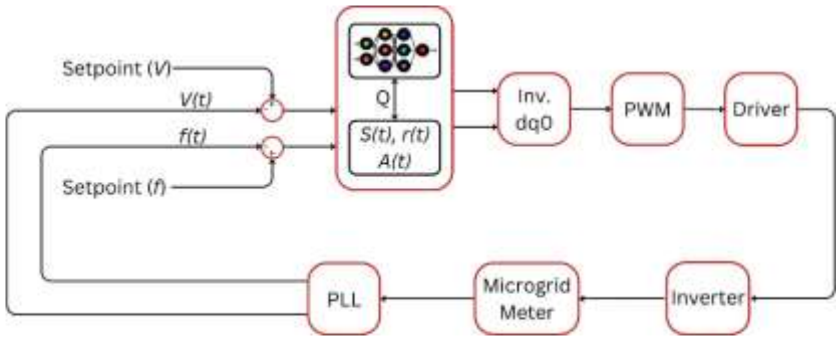

FIGURE 2. Illustration of the DRL training method

ISSN: 2252-4274 (Print)
ISSN: 2252-5459 (Online)

The DRL agent is trained to regulate the inverter output by interacting with a simulation environment. The controller is a DRL agent utilizing the TD3 algorithm. It observes bus-coupler status, voltage (pu), frequency (Hz), frequency error, and voltage error. To monitor error changes for each action, error derivatives are also observed. Additionally, integral error is tracked to monitor cumulative error. Therefore, the observation state $s(t)$ can be represented as follows:

$$\boldsymbol{s}(t) = [V(t) \quad f(t) \quad e_f(t) \quad e_v(t) \quad \dot{e}(t) \quad \int e(t)]^T \tag{1}$$

$V(t)$, $f(t)$, and all observed error values are in continuous observation states. The DRL agent's actions at time t include the inverter's direct d_i and quadrature q_i frame of the $dq0$ function, with the 0 remaining null due to the system's balanced state. During training, the reward function is defined as in equation:

$$R(t) = 1 - (0.05|e_f(t-1)|) - (|e_v(t-1)|) - L_p(t) \tag{2}$$

where e_f and e_v are the frequency and voltage error values deviating from their setpoints based on the agent's previous action. $L_p(t)$ is a breach limit penalty set at 1000, triggered if the frequency falls outside 49.5-50.5 Hz or the voltage (pu) exceeds 0.98-1.02, as shown in equation:

$$L_p(t) = \begin{cases} 1000 & if\ 49.5 > f > 50.5\ or\ 0.98 > v > 1.02 \\ 0 & else \end{cases} \tag{3}$$

The discount factor for future rewards is expressed as,

$$G(t) = \sum_{i=t}^{n} \gamma^{i-t} R_i \tag{4}$$

where, $G(t)$ represents the expected cumulative reward starting from time t, with γ set to 0.99. Further, the loss function is defined as,

$$\boldsymbol{L}(\theta) = \boldsymbol{E}\left[\left(Q(s_t, a_t|\theta) - (R_t + \gamma.\min(Q(s_{t+1}, a_{t+1}|\theta')))\right)^2\right] \tag{5}$$

where, $\boldsymbol{E}$ encompasses all possible observed states, θ are the parameters of Q-network, and θ' are the parameters of the target Q-network. Additionally, the exploration rate for action $a(t)$ defined as,

$$a(t) = \pi(s_t|\theta_{actor}) + \mathcal{N}(0, \sigma) \tag{6}$$

where, $\pi(s_t|\theta_{actor})$ is the deterministic action taken by the actor, $\mathcal{N}(0, \sigma)$ is the Gaussian noise with mean of 0 and standard deviation σ of 0.24. All the hyperparameters for DRL Agent training was summarized in Table 1.

TABLE 1. DRL Agent's hyperparameter for training session

Hyperparameter	Symbol	Value
Policy Update Frequency	—	2
Target Smooth Factor	τ	1e-3

Hyperparameter	Symbol	Value
Mini-Batch Size	—	256
Experience Buffer	—	8e5
Discount Factor	γ	0.99
Exploration Model Mean	—	0
Exploration Model Standard Deviation	σ	0.24
σ **(Decay)**	—	2.5e-6
σ **(Minimum)**	σ_{min}	2%
Target Policy Smooth Model (δ) **Mean**	—	0
δ **(Standard Deviation)**	σ_{target}	0.216
σ_{target} **(Decay)**	—	2.5e-6

2.3 EXPERIMENTAL SETUP

To verify the simulation results, the trained DRL controller is deployed onto the physical inverter system. As for the hardware setup, the inverter circuit, is constructed based on H-bridge topology. The voltage regulator is implemented on a microcontroller interfacing with the gate driver. Subsequently, the trained agent is deployed into an embedded processing unit, which receives voltage feedback and generates PWM signals. Furthermore, the inverter's output waveform is analyzed using an oscilloscope, as presented in Figure 3, to assess voltage stability, harmonic distortion, and response to load variations. The results are compared with simulation data to confirm the effectiveness of the DRL-based control strategy.

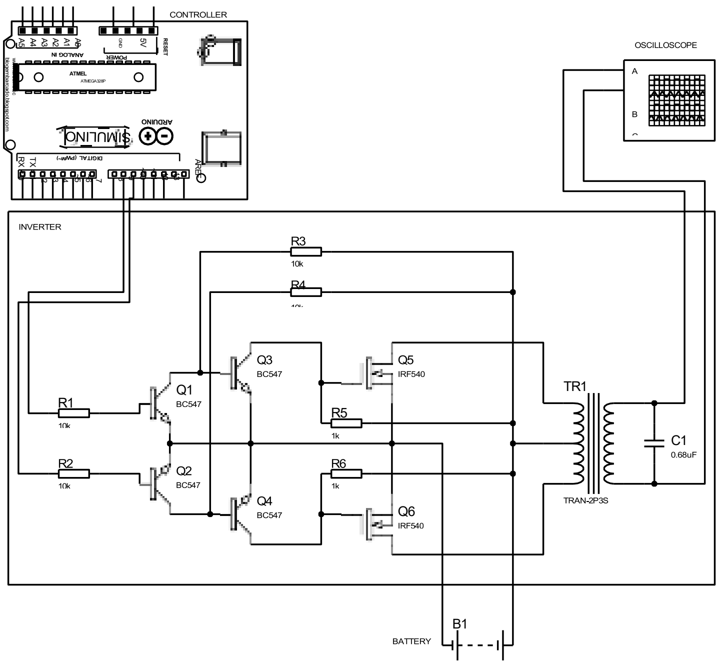

FIGURE 3. Hardware setup of the DRL-based single-phase inverter for experimental validation. The system includes the inverter circuit, control hardware, and measurement instruments.

The specifications of the inverter used in the laboratory-scale verification are provided in Table 2. This table outlines the key parameters of the inverter, including its input voltage range, maximum capacity, power factor, idle current, output voltage, output frequency, and output type. Additionally, the oscilloscope setup used for measurements is detailed, listing important attributes such as the number of channels, bandwidth, sampling rate, input resistance, sensitivity, and accuracy for voltage and

ISSN: 2252-4274 (Print)
ISSN: 2252-5459 (Online)

frequency. These specifications ensure accurate performance monitoring and verification during the experiments.

TABLE 2. Specifications of the inverter verified on a laboratory scale, along with the oscilloscope setup for measurements

Specification	Inverter	Oscilloscope
Input Voltage	12 - 24 VDC	-
Max. Capacity	500 VA	-
Power Factor (PF)	0.8	-
Idle Current	0.9 - 1 A	-
Output Voltage	220 VAC ± 3%	-
Output Frequency	50 Hz ± 0.5	-
Output Type	Modified Sine Wave	-
Channels	-	2
Bandwidth	-	100 MHz
Sampling Rate	-	1 GSa/s
Input Resistance	-	1 MOhm
Sensitivity	-	50 mV – 500V

3. RESULTS

3.1 DRL TRAINING RESULTS

Prior to experimental validation, the DRL-based inverter controller was trained in a simulated environment. The results demonstrated that the trained agent successfully regulated the inverter output, maintaining a stable 220 V_{rms}, 50 Hz sine wave despite load fluctuations. The frequency and voltage deviations were minimized through adaptive control, confirming the feasibility of the proposed DRL approach. Figure 4 summarized the mean absolute deviation of voltage and frequency under simulated environment, underlined the superiority of 2% exploitation rate as previously parameterized in Table 1.

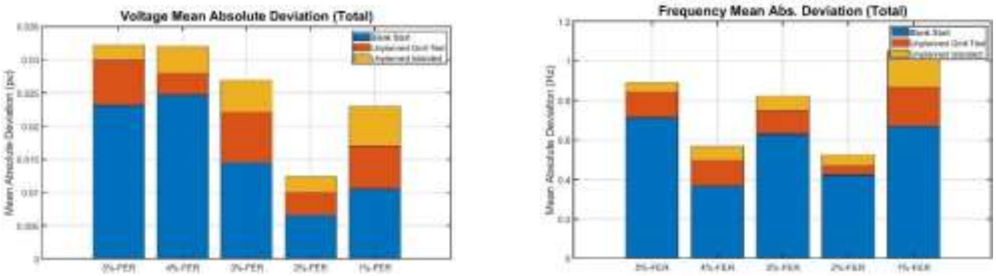

FIGURE 4. Mean absolute deviation of various experimental DRL Exploitation Rate

In Figure 5, we present the training episode reward, acquired by the DRL-Agent along its training session. Since the termination flag was not used during the override condition, the agent will eventually converge, albeit at varying time frames. As a result, at the end of training, the performance in terms of the power system is not significantly affected. Instead, the impact lies in the Final Exploitation Rate (FER) in regards to the available action range $A(t)$, which is influenced by the Exploration-Exploitation parameter.

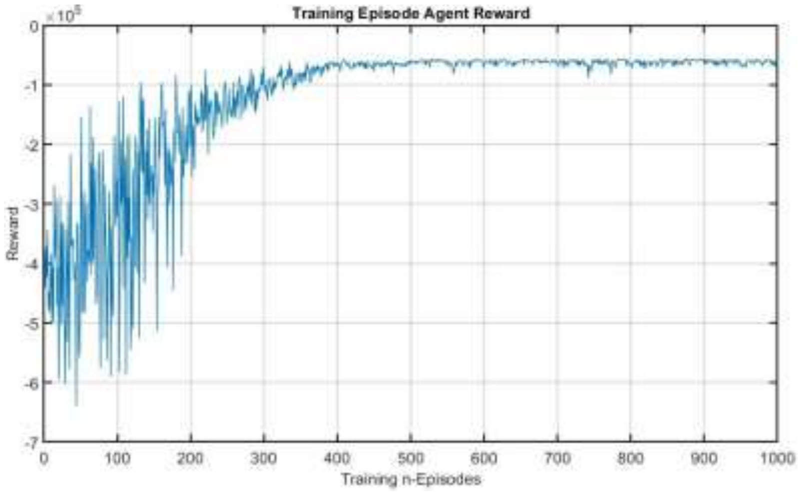

FIGURE 5. Training Episode DRL-Agent Reward

3.2 EXPERIMENTAL VALIDATION

The trained DRL controller was deployed on the hardware setup to verify real-world performance. The inverter successfully generated a pure sine wave output, as captured by the oscilloscope in Figure 6. The measured output voltage remained at 220 V_{RMS}, with a frequency deviation of less than 0.5 Hz, even under dynamic load conditions.

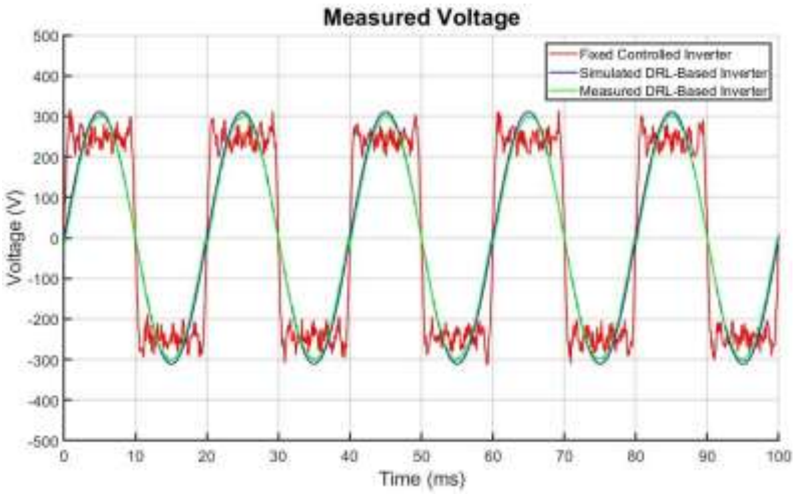

FIGURE 6. Verification results along with the simulation result

To evaluate total harmonic distortion, frequency spectrum analysis is introduced, and the system response was observed. As shown in Figure 7, the DRL-based controller effectively adjusted the output frequency in 50 Hz despite sudden variations or load fluctuations, preventing significant voltage sag or overshoot.

ISSN: 2252-4274 (Print)
ISSN: 2252-5459 (Online)

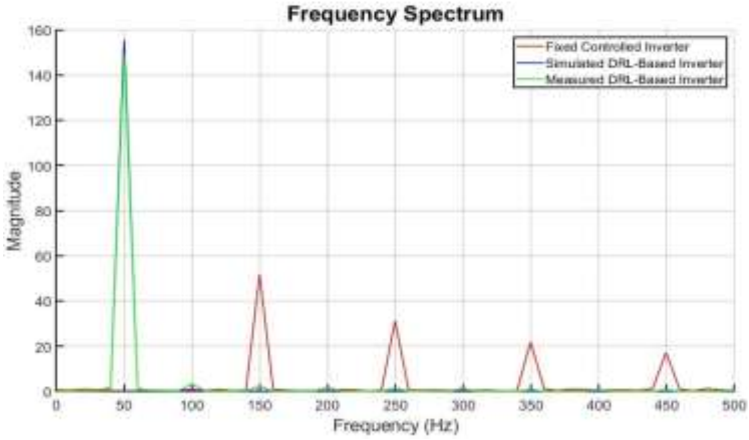

FIGURE 7. Showing result within Frequency Spectrum

3.3 PERFORMANCE COMPARISON

The following Table 3 presents a comparison between fixed controlled and DRL controlled systems in terms of Signal to Noise Ratio (SNR), Total Harmonic Distortion (THD), and Time-domain Metrics (VAC RMS). The table highlights the performance differences between the two control methods, providing a clear overview of their respective advantages and disadvantages in managing the power system's stability and efficiency.

TABLE 3. Comparison of Signal to Noise Ratio, Total Harmonic Distortion (THD), and Time-domain Metrics between Fixed and DRL Controlled systems

Metric	Fixed Controlled	DRL Controlled
Signal to Noise Ratio	25.27 dB	6.96 dB
THD	16.74%	7.56%
Time-domain Metrics	210.98 V_{AC} (RMS)	219.8 V_{AC} (RMS)

The key findings from the comparison between fixed controlled and DRL controlled systems are quite significant. The signal to noise ratio (SNR) for the fixed controlled system is much higher at 25.27 dB compared to 6.96 dB for the DRL controlled system, indicating a cleaner signal in the fixed controlled setup. However, the DRL controlled system excels in total harmonic distortion (THD), with a lower percentage of 7.56% compared to 16.74% in the fixed controlled system, suggesting better waveform quality. Additionally, the DRL controlled system shows a slightly stable voltage regulations with 219.8 V_{RMS}, compared to 210.98 V_{RMS} for the fixed controlled system, demonstrating improved voltage regulation. These findings highlight the trade-offs between the two control methods and underscore the potential benefits of using DRL for enhanced performance in power systems.

4. DISCUSSION

The results from both simulation and experimental validation confirm that a DRL-based control strategy can effectively stabilize a single-phase inverter for microgrid islanded applications. The key advantages and implications of this approach are discussed below.

4.1 PERFORMANCE ANALYSIS

The proposed DRL-based inverter demonstrated stable voltage and frequency regulation, maintaining 220 V_{RMS} at 50 Hz under varying load conditions. Moreover, the measured Total Harmonic Distortion (THD) remained below 8%, which indicates that the DRL-based approach is capable of generating a high-quality output waveform.

4.2 ADAPTABILITY AND FUTURE IMPROVEMENTS

The results suggest that deep reinforcement learning offers a promising alternative to conventional inverter control techniques, particularly for systems operating under uncertain and fluctuating load conditions. However, several areas for improvement remain:

- Training Generalization: While the DRL agent performed well under tested conditions, further training with a wider range of load profiles could enhance its robustness in real-world scenarios.
- Computational Efficiency: Deploying DRL controllers in embedded systems requires optimizing inference speed to minimize latency. Future work could explore lightweight neural network architectures for real-time processing.
- Hybrid Control Strategies: Combining DRL with conventional control methods, such as fuzzy logic or model predictive control (MPC), could further improve stability and response time under extreme operating conditions.

4.3 PRACTICAL APPLICATIONS

The proposed DRL-based inverter presents a viable solution for microgrid and off-grid power systems, where cost constraints often limit access to high-quality power electronics. Potential applications include:

- Renewable Energy Systems: Inverters for solar and wind power integration, where fluctuating generation requires adaptive control.
- Rural Electrification: Low-cost power solutions for remote areas, reducing dependency on expensive commercial inverters.
- Industrial Power Backup: Smart inverters for uninterruptible power supplies (UPS) with improved dynamic response to load changes.

Overall, the study demonstrates that DRL-based control can significantly enhance inverter performance while reducing system cost and complexity, making it a compelling alternative for next-generation power electronics.

5. CONCLUSION

This study demonstrated the feasibility of a low-cost, single-phase inverter controlled by a deep reinforcement learning (DRL) agent. The results confirmed that the DRL-based inverter successfully maintained a stable 220 V_{RMS}, 50 Hz output voltage under varying load conditions, achieving performance comparable to commercial high-cost inverters.

ISSN: 2252-4274 (Print)
ISSN: 2252-5459 (Online)

The study highlights the potential of DRL-based control in power electronics, particularly for microgrid islanded configurations, renewable energy systems, and rural electrification. Future work will focus on improving training generalization, optimizing computational efficiency, and exploring hybrid control strategies to enhance real-time performance and adaptability.

Overall, the findings suggest that DRL-based control provides a robust, adaptive, and cost-efficient solution for next-generation power inverters, paving the way for wider adoption in microgrid and distributed energy applications.

ACKNOWLEDGEMENT

This research was funded by the Anggaran DIPA Badan Layanan Umum Universitas Sriwijaya for the 2024 Fiscal Year, under No. SP DIPA-023.17.2.677515/2024, dated November 24th, 2023, in accordance with SK Rektor No. 0013/UN9/LP2M.PT/2024, dated May 20th, 2024. The authors express their gratitude to Universitas Sriwijaya for the financial support provided for this study.

REFERENCES

[1] Z. Shuai, Y. Peng, J. M. Guerrero, Y. Li, and Z. J. Shen, "Transient Response Analysis of Inverter-Based Microgrids under Unbalanced Conditions Using a Dynamic Phasor Model," *IEEE Transactions on Industrial Electronics*, vol. 66, no. 4, pp. 2868–2879, Apr. 2019, doi: 10.1109/TIE.2018.2844828.

[2] M. Cucuzzella, G. P. Incremona, M. Guastalli, and A. Ferrara, "Sliding mode control for Maximum Power Point Tracking of photovoltaic inverters in microgrids," in *2016 IEEE 55th Conference on Decision and Control, CDC 2016*, 2016. doi: 10.1109/CDC.2016.7799395.

[3] S. K. Sarkar, F. R. Badal, and S. K. Das, "A comparative study of high performance robust PID controller for grid voltage control of islanded microgrid," *Int J Dyn Control*, vol. 6, no. 3, pp. 1207–1217, 2018, doi: 10.1007/s40435-017-0364-0.

[4] R. Aghatehrani and R. Kavasseri, "Sensitivity-analysis-based sliding mode control for voltage regulation in microgrids," *IEEE Trans Sustain Energy*, vol. 4, no. 1, pp. 50–57, 2013, doi: 10.1109/TSTE.2012.2197870.

[5] R. K. Chauhan, B. S. Rajpurohit, R. E. Hebner, S. N. Singh, and F. M. G. Longatt, "Design and analysis of PID and fuzzy-PID controller for voltage control of DC microgrid," in *Proceedings of the 2015 IEEE Innovative Smart Grid Technologies - Asia, ISGT ASIA 2015*, 2015, pp. 1–6. doi: 10.1109/ISGT-Asia.2015.7387019.

[6] D. L. Nguyen and H. H. Lee, "Fuzzy PID Controller for Accurate Power Sharing in DC Microgrid," in *Lecture Notes in Computer Science (including subseries Lecture Notes in Artificial Intelligence and Lecture Notes in Bioinformatics)*, 2019, pp. 71–80. doi: 10.1007/978-3-030-26969-2_7.

[7] S. Yaghoobi and H. Mojallali, “Tuning of a PID controller using improved chaotic Krill Herd algorithm,” *Optik (Stuttg)*, vol. 127, no. 11, pp. 4803–4807, 2016, doi: 10.1016/j.ijleo.2016.01.055.

[8] N. F. P. Dinata, M. A. M. Ramli, M. I. Jambak, M. A. B. Sidik, and M. M. Alqahtani, “Designing an optimal microgrid control system using deep reinforcement learning: A systematic review,” *Engineering Science and Technology, an International Journal*, vol. 51, 2024, doi: 10.1016/j.jestch.2024.101651.

[9] M. Wadi, A. Shobole, W. Elmasry, and I. Kucuk, “Load frequency control in smart grids: A review of recent developments,” 2024. doi: 10.1016/j.rser.2023.114013.

[10] W. Pattaraprakorn, P. Bhasaputra, and J. Pattanasirichotigul, “Impacts of PV power plants on distribution grid for voltage stability and economic values,” in *ECTI-CON 2015 - 2015 12th International Conference on Electrical Engineering/Electronics, Computer, Telecommunications and Information Technology*, 2015. doi: 10.1109/ECTICon.2015.7206935.

[11] I. Alhamrouni, M. A. Hairullah, N. S. Omar, M. Salem, A. Jusoh, and T. Sutikno, “Modelling and design of PID controller for voltage control of AC hybrid micro-grid,” *International Journal of Power Electronics and Drive Systems*, vol. 10, no. 1, pp. 151–159, 2019, doi: 10.11591/ijpeds.v10n1.pp151-159.

[12] M. Regad, M. Helaimi, R. Taleb, A. M. Othman, and H. A. Gabbar, “Frequency control of microgrid with renewable generation using pid controller based krill herd,” *Indonesian Journal of Electrical Engineering and Informatics*, vol. 8, no. 1, pp. 21–32, 2020, doi: 10.11591/ijeei.v8i1.1291.

[13] D. Feldmann and R. V. de Oliveira, “Operational and control approach for PV power plants to provide inertial response and primary frequency control support to power system black-start,” *International Journal of Electrical Power and Energy Systems*, vol. 127, 2021, doi: 10.1016/j.ijepes.2020.106645.

ISSN: 2252-4274 (Print)
ISSN: 2252-5459 (Online)